Specification, Design, and Test of Aircraft Engine Isolators for Reduced Interior Noise

J F Unruh*
Southwest Research Institute San Antonio, Texas

Improved engine vibration isolation was proposed to be the most weight and cost efficient retrofit structure borne noise control measure for single engine general aviation aircraft A study was carried out with three objectives: 1) to develop an engine isolator design specification for reduced interior noise transmission, 2) to select and/or design candidate isolators to meet a 15 dB noise reduction design goal, and 3) to carry out a proof of concept evaluation test A coupled analytical and empirical model was used to develop an engine isolator dynamic properties design specification for reduced noise transmission Candidate isolators were chosen from available products and retrofitted to a test aircraft, and a laboratory based test procedure was used to simulate engine induced noise transmission in the aircraft for a proof of concept evaluation test Several candidate isolator configurations were evaluated relative to the original equipment isolators Analyses of the resulting noise transmission data show that overall maximum interior noise level reductions on the order of 10 dB were realized from the candidate isolators, and the noise transmission model used in the isolator design specification was quite adequate for evaluating trends in improved isolation for known isolator dynamic properties

Nomenclature

A_B	= base excitation acceleration
A_m	= supported mass acceleration
CF	= force level correction factor
f	= harmonic frequency
f_{BAND}	= one third octave frequency band
g	= acceleration due to gravity
i	= complex number $\sqrt{-1}$
K	= parameter defined as kg/ω^2
K_A	= isolator axial stiffness frequency dependent
$\bar{K}_A$	= isolator axial stiffness at 100 Hz
K_A^s	= isolator axial static stiffness
L_R	= ratio of isolator radial to axial stiffness
P1,P2 P3	= microphone locations
rpm	= engine speed
T	= transmissibility
W	= supported test weight
X_B	= base excitation displacement
X_e	= engine maximum static displacement
X_m	= supported mass displacement
β	= frequency hardening parameter and critical damping ratio
η	= material loss factor
θ	= phase angle in general
θ_x	= engine rotation about X axis
ω	= circular frequency $2\pi f$

Introduction

OVER the past several years an active research program has been carried out to gain a better understanding of the sources of structure borne interior noise paths of propaga tion and methods of noise control in lightweight general aviation aircraft During the conduct of the program a single engine lightweight aircraft was employed as a ground test vehicle in a series of engine attached and detached engine running tests to determine the relative levels of structure borne and airborne noise [1,2] From the ground test results it was concluded that engine induced structure borne noise was equal to or greater than airborne noise transmission and therefore a concentrated effort in the area of developing structure borne noise control measures would be necessary if overall interior noise of the aircraft were to be reduced

A structure borne interior noise prediction model of the test aircraft was developed using a structural acoustic finite element modeling procedure [3] A comparison of predicted results to laboratory measured aircraft response and to engine running data showed that structural acoustic coupling i e fuselage flexibility had a strong influence on the fundamental cabin acoustic resonances and provided the major low frequency path for engine induced structure borne noise From analytical model studies[4] it was concluded that the most effective and lightweight noise control measure would appear to be improved engine vibration isolation

Data on the effectiveness of improved engine vibration isolation for reduced structure borne noise transmission was not available in the literature and therefore the efforts of the program were directed towards a study of this potential noise control measure A laboratory test procedure was developed to simulate engine induced structure borne noise transmission in the test aircraft via electrodynamic shaker excitation [5] Analysis of the interior sound pressure level transfer function data for a series of isolators with varying mechanical properties showed as expected, that decreasing the engine support frequencies results in reduced structure borne noise transmission out to approximately 150 Hz Beyond 150 Hz isolation levels off and appears to decrease somewhat above 600 Hz It was concluded that elastomeric isolators do not respond as constant parameter single degree of freedom components but, rather, exhibit responses characteristic of components with frequency dependent properties A procedure was then developed for the evaluation of engine vibration isolators for reduced structure borne transmission by coupling analytical models of the engine, vibration isolators and engine mount structure to an empirical model of the fuselage [6] By comparison of predicted structure borne noise transmission to laboratory based measurements it was observed that isolator stiffness was a strong parameter governing the noise transmission while isolator damping was a much weaker parameter It was also found that for the test aircraft moderate changes to the lightweight high strength engine mount structure did not affect the transmission

Received Feb 4 1983; revision received Jan 15 1984

Staff Engineer Department of Engineering Mechanics Senior Member AIAA

phenomena The study indicated that the modeling procedures were adequate to judge the relative performance of candidate isolators for the purpose of retrofit isolator design if the mechanical properties of the isolators were known [6]

The objective of the present study was to use the previously developed structure borne noise transmission model as an isolator design tool to predict the required isolator characteristics for a desired level of noise reduction relative to the performance of the original equipment isolators Improved isolators were then to be built and tested for a proof of concept evaluation

The physical components of the structure borne noise transmission model and the corresponding mathematical coupling procedures used in the previous and present investigations are presented in detail in Refs. 5 and 6 In the sections to follow the isolator design specifications developed for this study will be discussed along with the selection and mechanical properties evaluation of candidate isolators chosen to meet a design objective of 15-dB reduction in structure borne noise transmission Thereafter the laboratory based test setup used to evaluate the candidate isolators along with corresponding test results and correlation of test results to the design model predictions will be given In depth discussion of all aspects of the program may be found in Ref 7

Isolator Design Specification

When armed with a structure borne noise transmission prediction model, how does one specify the required isolator mechanical properties to achieve a desired noise reduction goal and what are the overall aircraft design penalties or constraints? The present study was aimed at answering these questions with as much realism for an in flight design/evaluation as possible within the budgetary constraints of the program To this end the design specification and evaluation was limited to laboratory simulations of expected in flight engine excitation This approach was also prompted by the lack of in flight or engine running ground test procedures that would allow determination of reduced levels of structure borne noise in the presence of a high level of airborne noise transmission, i.e reliable source separation procedures

Engine Excitation

The engine running engine attached/detached data obtained during a previous investigation[2] was used to establish a realistic engine source The engine running structure borne noise spectra provide a realistic measure of the relative importance of each one third octave band level to the overall spectrum sound pressure level During flight the test aircraft engine operates in a speed range of 2100 to 2700 rpm Using the measured structure borne interior noise levels at an engine speed of 2160 rpm, the shaker force level for the configuration shown in Fig 1 was adjusted such that the predicted one third octave sound pressure level (SPL) data using the original equipment isolators (with assumed dynamic to static factors) matched the measure interior levels The measured structure borne noise spectra at 2160 rpm are given in Fig 2 The input force spectrum consists of harmonics of 18 Hz (2160/120) out to 1000 Hz Each force level is assigned to a harmonic, which can then take on various spectrum frequencies depending on the desired engine speed

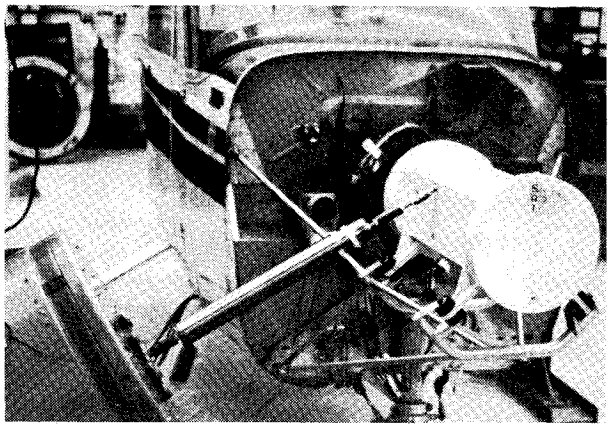

Fig 1 Laboratory test setup

From aircraft performance charts[8] the engine torque at a given altitude is related to engine rpm When the torque level at 2160 rpm (23 750 N/cm) is used as a reference assuming the dynamic engine forces are proportional to the engine static torque levels a force level correction factor of the form

$$CF = 3392 - 5166/\text{rpm} \tag{1}$$

results for a reference altitude of 762 m Here we see that at an engine speed of 2640 rpm the force levels increase by 44% over those at 2160 rpm

Design Parameters

Engine Speed

While there exist an infinite number of engine speeds in the aircraft operating range, for the purpose of this study the five engine speeds 2160, 2280, 2400 2520, and 2640 rpm were used exclusively The corresponding engine 1/2 rpm harmonics are respectively 18 19, 20, 21, and 22 Hz As will be shown later the maximum overall sound pressure level (OASPL) did not always occur at the highest engine speed, and therefore a series of evaluations at various engine speeds was necessary to obtain an estimate of the peak SPL

Engine Motion

The engine motion of primary importance to the designer may be that due to static torque rotation There are other possible engine motions; however we consider only the engine torsional rotation θ_x With engine torque expressed in terms of engine speed,[8] an expression was developed to relate engine speed and isolator stiffness in the form

$$\theta_x = (37\ 454 - 57{,}048/\text{rpm})/K_A^s \tag{2}$$

where rpm is the engine speed, and K_A^s is the axial static stiffness of one of the four engine isolators in N/cm For the original equipment isolators $K_A = 4640$ N/cm At engine speeds of 2160 and 2640 rpm, the engine static rotations are, respectively, 0 0024 and 0 0034 rad or 0 122 and 0 173 cm (based on a maximum distance, engine c g to cowling, of 50 8 cm) Noting that the maximum engine static torque is produced at the highest engine speed of 2640 rpm, the engine maximum static displacement X_e, at a rotational arm of 50 8 cm may be expressed in terms of the isolator static axial stiffness K_A^s as

$$X_e = 805/K_A^s \tag{3}$$

where X_e is expressed in centimeters and K_A^s in N/cm This expression is used directly to obtain a relative measure of the expected engine deflection for a candidate isolator

Overall dynamic motion of the engine was also taken into consideration; however, the resulting dynamic motions were small in comparison to the static torque loading deflection [7]

Isolator Mechanical Properties

The potential frequency dependence of an isolator was included in the design model by postulating a maximum allowable axial isolator stiffness vs frequency envelope of the form

$$K_a = \bar{K}_A \begin{cases} 1\ 0 & f \le 100 \\ [100 - \beta(\beta-1)f^2/10\ 000]/99 & 100 \le f \le 1000 \end{cases} \tag{4}$$

where β is a parameter in the range from 1 to 10 From the measured stiffness properties of a soft rubber isolator (22002 1) it was found that a minimum value of β would be on the order of two to three Measured values of β for several isolators are given in a following section The parameter denoted as L_R (called L ratio) was used to specify the ratio of radial to axial stiffness The use of the L ratio is consistent with isolator manufactures's static stiffness product specifica tions The use of the L ratio is normally conservative when specifying isolator dynamic properties [7]

Previous studies[6] showed that the isolator material loss factor η was a weak parameter with respect to noise trans mission. In the present study, the isolator material loss factor was considered to be frequency independent and employed as a structural loss factor

Parametric Design Curves

The input parameters to the structure borne noise trans mission model are as follows: 1) engine speed (rpm) 2) isolator axial dynamic stiffness ($\bar{K}_A$) 3) ratio of radial to axial stiffness (L_R) 4) ratio of stiffness at 1000 Hz to stiffness at 100 Hz (β) and 5) isolator material loss factor (η)

Upon entry of these parameters into the transmission model, expected maximum (based on maximum response from three interior microphones P1 P2 and P3) sound pressure level one third octave spectra (both unweighted and A weighted) were generated Maximum OASPL and OASPL(A) values were determined from spectra generated at the five engine speed settings with the maximum OASPL and OASPL(A) not always occurring at the same engine speed

The isolator axial dynamic stiffness was varied in the range from $\bar{K}_A = 438$ to 7000 N/cm with corresponding engine static torque deflections of 3 68 to 0 230 cm based on an isolator static to dynamic ratio of 2 0 The L ratio was varied from 0 25 to 8 0 and as will be seen is one of the stronger parameters except for $\bar{K}_A$ Material loss factor η was varied in the range of 0 05 up through 0 45 and was a very weak parameter

A series of isolator design curves were developed based on the above range of parameters and several are presented in Figs 2 5 In Fig 3 predicted maximum unweighted OASPL levels are given vs L ratio for nominal values of β and η and at various values of isolator axial stiffness Depending on the stiffness value $\bar{K}_A$ an optimum value of L_R appears to be around the value of 2 0 The unweighted interior noise levels were insensitive to the specified isolator frequency depen dence since peak spectrum levels occur in the lower frequency range where β has little or no effect

In Figs 4 and 5 data are presented with the A weighted OASPL values as the dependent design variable As shown in Fig 4 the optimum L ratio is not around 2 0 but would be closer to 0 25 i e the isolator needs to be weaker in the radial direction than in the axial direction by a factor of 4 0 At the higher values of support stiffness considerable variations of OASPL with L ratio occur Physical reasons for these variations will be discussed below In Fig 5 the effects of variation of β on the expected A weighted OASPL's are shown As can be seen an increase in β results in an increase in OASPL(A) with more pronounced effects at the higher support stiffnesses The general trend is expected since the A weighted network reduces the low frequency components of the response Again at the higher support stiffness increased sensitivity occurs

The rather odd noise transmission behavior occurring at the higher isolator stiffness as is shown in Figs 4 and 5 is at tributed to a decrease in fuselage stiffness at the higher frequencies Recall that a driven mass sees not only the spring stiffness of its isolator support but also the stiffness of the base to which the isolator is attached In this case the fuselage stiffness at the engine mount attach points is of interest A general rule of thumb is to supply a base stiffness 10 times that of the isolator Review of the test aircraft fuselage stiffness at the engine mount attach points showed that this can be quite difficult to achieve in lightweight aircraft con

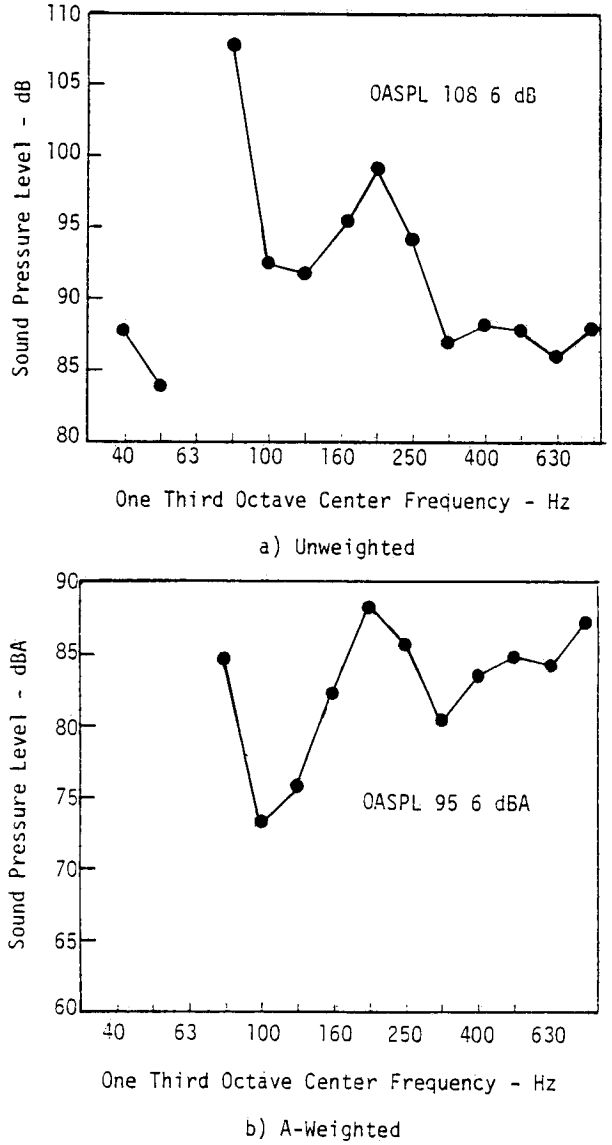

Fig 2 Measured structure borne noise levels 2160 rpm

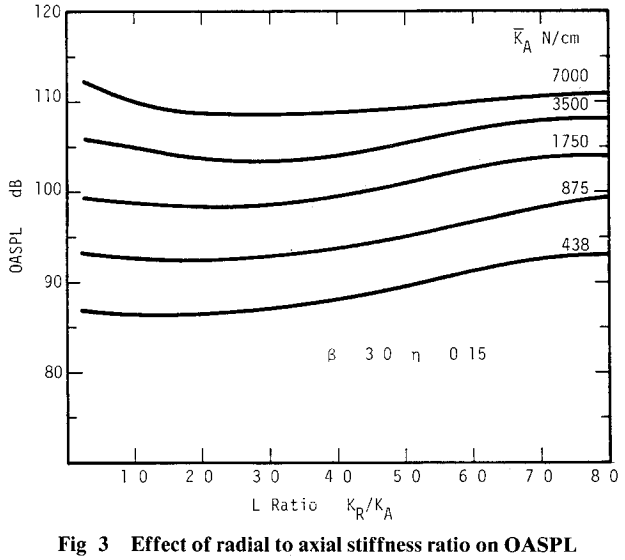

Fig 3 Effect of radial to axial stiffness ratio on OASPL

struction In fact achieving a 10:1 stiffness ratio in all support directions may be impossible if the isolators exhibit a frequency hardening effect such as for $\beta = 3$

Design Objective

The maximum OASPL and OASPL(A) for the original equipment isolators occurred at an engine speed of 2640 rpm at levels of 114 dB and 105 dB(A) respectively A design objective was set at reducing these predicted maximum SPL levels by 15 dB; thus the objective could be met by reducing the structure borne noise levels to 99 dB and 90 dB (A) From the design curves given in Figs 3 5 it can be seen that a rather wide selection of possible isolator parameters is allowed as long as the isolator axial dynamic stiffness is 1750 N/cm or less We may also note that it is the unweighted spectrum that will control the isolator design as long as the L ratio is somewhat less than 5 0 A reasonable design improvement could be expected by selecting $\bar{K}_A = 1750$ N/cm $L_R = 2\ 0$ $\beta = 3\ 0$ and $\eta = 0\ 15$ resulting in OASPL levels of 97 8 dB and 84 2 dB(A) This design choice results in a 16 dB or 20 dB(A) decrease in expected interior noise levels The penalty for this increase in transmission loss is a predicted increase in engine motion from 0 172 to 0 919 cm due to static torque

Configurations and Mechanical Properties

Physical Constraints

The physical constraints placed on the selection of candidate isolator configurations arise from two sources those due to geometric constraints, i e compatibility with the existing engine and engine mount structure and those associated with the engine static preloads which must be supported by the isolator For the laboratory based dummy engine design several possible candidate isolator configurations could be found from existing stock items available from isolator manufacturers which would require only a minimum of refixturing of existing hardware The only isolator preload of interest in the laboratory based evaluation is that due to the engine deadweight With a dummy engine weight of 170 Kg the candidate isolators will be subjected to axial and radial preloads in the range of 250 to 340 N For an inflight design the engine static torque and thrust preloads on the isolators must also be considered; however these preloads were not included in the laboratory simulation

Selection of Candidate Configurations

The selection of candidate isolators which would satisfy the above constraints and lie within the acceptable range of isolator parameters was based on suggestions from isolator manufacturers and the isolator static properties given in available product literature It should be realized that available isolator data are at most static unidirectional load deflection curves or a specification of maximum rated load and corresponding deflection at that load To satisfy the requirement that $\bar{K}_A$ be less than 1750 N/cm would conservatively require that the isolator static stiffness K_A^S be equal to or less than 875 N/cm when considering a dynamic to static ratio of 2 0 With an isolator axial preload of 340 N the preload deflection would be 0 386 cm

A photograph of the isolators used in the present investigation is given in Fig 6 Three of the isolators denoted as Rigid 3006H, and 22002 1 were isolators used previously to develop the transmission model [6] The rigid configuration is a solid steel isolator which provides a rigid link between the engine and the engine mount structure The only local compliance in the system would come from the isolator attachment lugs The 3006H configuration consists of the original equipment tube form mounts fitted with a pair of steel collars to pick up loads in the axial direction The 22002 1 configuration consists of the soft rubber mount for which

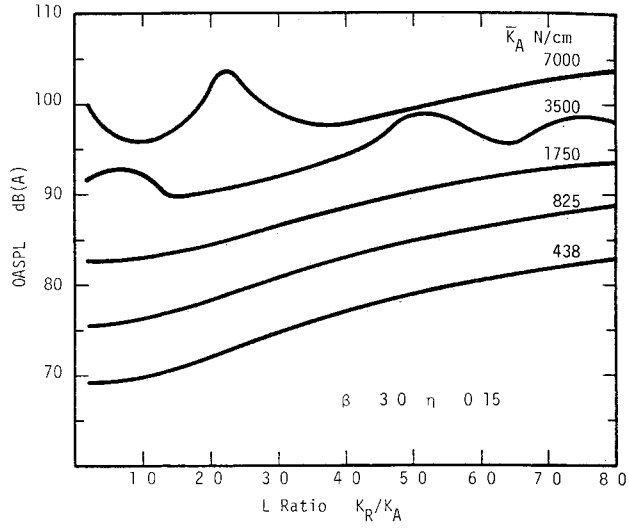

Fig 4 Effect of radial to axial stiffness ratio on OASPL, A wt

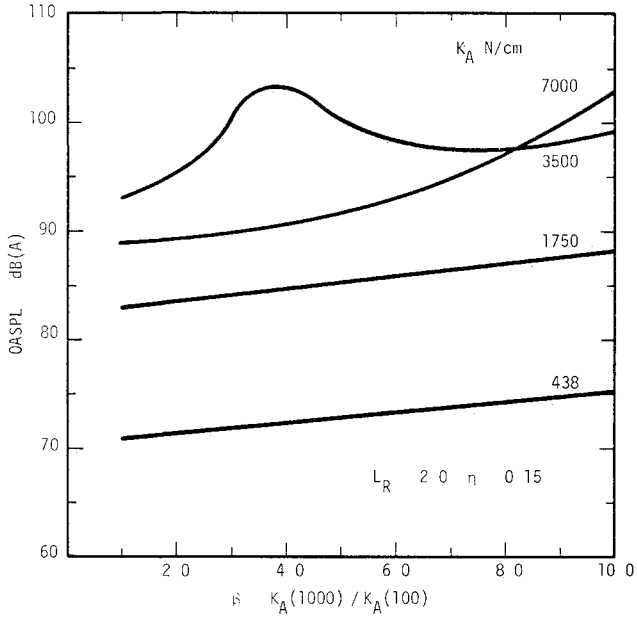

Fig 5 Effect of isolator frequency dependence on OASPL A wt

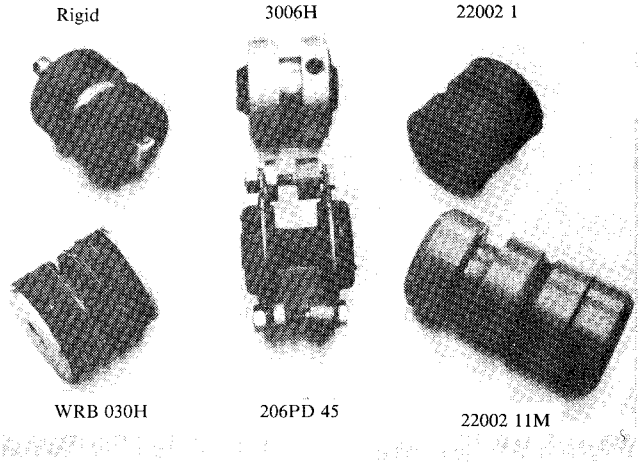

Fig 6 Isolator configurations

the dummy engine isolator attachment lugs were originally designed The remaining three isolator configurations were specifically selected to meet the program design objectives

The WRB 030M configuration consists of a pair of modified WR4 030 and WB4 030 ring and bushing mounts The mounts are rated at a maximum load of 157 N each thus having marginal preload capacity The ring mounts were modified by removing a set (12 each) of the fingers on one side of the mount to allow sufficient penetration of the bushing mount into the engine attachment lug to insure proper alignment during installation

The 22002 11M isolator configuration is a modification of the original soft rubber isolator 22002 1 The 22002 1 was modified to increase the isolator axial rubber wall " i e the length of elastomer in axial compression by adding two additional bushings. The isolator components were cast with a low durometer high damped elastomer The manufacturer's rated loads of the 22002 1 isolator are 267 and 178 N in the axial and radial directions, respectively Thus it was felt that the modified design would be quite adequate in the axial direction with marginal static load capability in the radial direction

A pair of multiplane mounts was used in the 206PD 45 isolator configuration The manufacturer's rated load for one of the mounts is 200 N at a deflection of 0 476 cm with the axial and radial stiffnesses being nearly equal From the rated load deflection data the isolator expected static stiffness would be $K_A = 840$ N/cm which just meets the static stiffness criteria

Static Load Deflection Characteristics

Static load deflection data for each of the three candidate isolator configurations were obtained for unidirectional and bidirectional loading The data were used to obtain a measure of the effects of bidirectional loading on the isolators and isolator static stiffness values for correlation to measure structure borne interior noise transmission data The static load-deflection data were obtained using a series of dead weight loadings in the range from 0 to 356 N The bidirectional loading consisted of a static 356 N transverse load to simulate maximum expected static preload of the opposite axis i e radial for loading in the axial direction etc The isolator static stiffness values in the 311 356 N load range are summarized in Table 1

During the static load tests a rapid axial stiffness increase in the WRB 030M configuration occurred indicating an overload of the elastomer and placing the isolator out of the acceptable static stiffness range (below 875 N/cm) The reduced strength of the isolator is partially attributed to the modifications that were made to accommodate its installation The 206PD 45 isolator configuration in the axial direction was quite unaffected by a radial preload; however the radial axis was quite sensitive to axial preload and nearly doubled in stiffness In general the isolator configurations were sensitive to off axis preloads exhibiting various trends both increasing and decreasing in stiffness [7]

It is of interest to note the effects of bidirectional preloads on the isolator static stiffness since bidirectional preloading of the isolators was not possible during the dynamic properties tests It is not known if bidirectional preloads produce similar effects in the isolator dynamic stiffness properties

Table 1 Isolator static stiffness values in 311 356 N load range

Isolator	Stiffness ~ N/cm Undirectional loading	Bidirectional loading, 356 N
WRB 030M		
Axial	1280	1350
Radial	2330	3500
22002 11M		
Axial	325	515
Radial	3500	1840
206PD-45		
Axial	650	650
Radial	935	1750

Dynamic Properties

As previously discussed at the onset of the present investigation it was felt that a successful isolator design would require data on the dynamic stiffness properties of the candidate isolators After searching the open literature such data were found to be for the most part nonexistent

Dynamic properties of the isolator configuration were determined using a base excitation seismic driven test configuration as is schematically shown in Fig 7 For the test setup the equation of motion is

$$(W/g)A_m + k(1+i\eta)(X_m - X_B) = 0 \tag{5}$$

where W is the weight of the supported mass g the gravitational acceleration k the unknown isolator stiffness η the unknown isolator material loss factor X_B the base excitation displacement and A_m and X_m the supported mass acceleration and displacement respectively For harmonic motion the transmissibility T may then be written as

$$T = (A_m/A_B) = \frac{K[((K-W)+\eta^2K)^2 + (\eta(K-W)-\eta K)^2]^{1/2}}{[(K-W)^2 + K^2\eta^2]} \exp[i\theta] \tag{6}$$

where

$$\tan\theta = \frac{[(K-W)-\eta K]}{[(K-W)+\eta^2 K]} \tag{7}$$

and $K = kg/\omega^2$

For a given transmissibility ratio T and phase angle θ between A_m and A_B the above expression may be solved for K and η For our purposes η is not a strong parameter and was obtained via the amplification ratio at the support mass resonance as

$$\eta = 1/[T^2 - 1] \tag{8}$$

using the above value of isolator loss factor throughout the frequency range of interest allowed the direct use of Eq (6) in an iterative way to determine the stiffness at any frequency The use of Eq (7) was found to yield very inconsistent results due to small changes in phase θ beyond the isolator support resonance

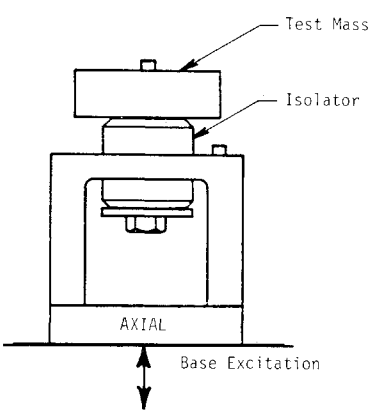

Fig 7 Dynamic properties test setup

Table 2 Isolator dynamic properties taken from test data

Isolator	$\bar{K}_A$, N/cm	L_R	β	η	X_e, cm	K^s_A, N/cm
Rigid[a]	52 535	8 0	1 0	0 0	0 015	52 535
3006H[b]	8 055	8 0	1 0	0 10	0 173	4 640
22002 1	4 115	0 98	2 3	0 10	0 368	2 190
WRB 030M	2 225	2.52	5 0	0 16	0 597	1 350
22002 11M	3 325	6 84	5 0	0 31	1 56	515
206PD 45	1,315	1 47	5 0	0 10	1 24	650

[a] Local engine mount compliance [b] Not tested; properties taken from product literature

Detailed transmissibility data for the 22002 1 WRB 030M 22002 11M and 206PD 45 isolator configurations are given in Ref 7 In general wave effects in the elastomers caused an apparent increase in stiffness at the higher frequencies, i e the β effect It was found that higher preloads tended to suppress wave effects and thus support masses near the ex pected installed isolator preloads were used during the dynamic tests for a majority of the isolators The isolator axial stiffness curves were fitted to the isolator stiffness design model [reference Eq (4)] by selecting $\bar{K}_A$ as the stiffness value at 100 Hz and determining the appropriate β value A sum mary of the isolator dynamic properties in terms of the design model parameters is given in Table 2

In general all the isolator configurations exhibited some degree of nonlinearity with respect to support mass weight (preload) and/or excitation amplitude; however within range of expected preload and excitation amplitudes the data listed in Table 2 are considered to be representative of the installed isolator properties The only exception is the effect of bidirectional static preload which is indicated by the static load deflection data presented in Table 1

Noise Transmission Tests

Test Setup

The wings empennage and interior trim were removed from the test aircraft shown in Fig 1 Three interior microphones were used in the aircraft One microphone P1 was positioned at the pilot's ear level a second, P2 at the copilot's ear level and a third, P3 midcabin at the passenger's ear level Maintaining identical positions of the interior response microphones P1 P2 and P3 throughout the model development and during the present investigation was felt to be most important owing to large spatial variations in cabin pressure levels that result from excitation of structural acoustic resonances[2] in the lower frequency region Engine excitation was provided by a 7100 N electrodynamic shaker attached to the engine via a load cell in the position shown in Fig 1 This excitation position introduces torsional oscillations of the engine, thereby providing a realistic engine excitation In order to simulate the full spectrum of engine 1/2 rpm harmonics a terminal peak sawtooth (linear ramp pulse) drive signal was used The signal was shaped with a series of filters to give a spectrum distribution representative of the design model spectrum To minimize direct shaker noise radiation the shaker face was covered with a lead blanket during data acquisition

Data Acquisition and Reduction

The shaker input force and the three interior microphone responses were recorded for each of the five engine speed settings on a 14 channel FM intermediate band magnetic tape for postdigital data analyses The data were then replayed into an analog to digital conversion system with antialiasing filters set at 1250 Hz and digitized at a rate of 4096 samples/s/ channel The data were organized into 1 s records and Fourier transformed to the frequency domain (bandwidth of resolution 1 0 Hz) A typical microphone response amplitude spectrum is given in Fig 8; as expected, the microphone response is rich in tonal response, reflecting the spectral content of the drive signal

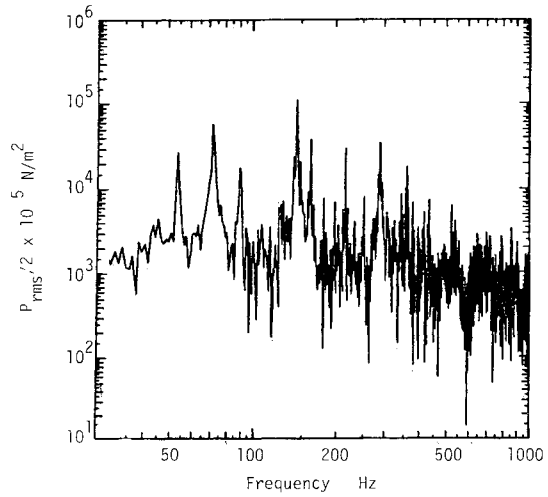

Fig 8 Typical pressure amplitude spectrum 2160 rpm

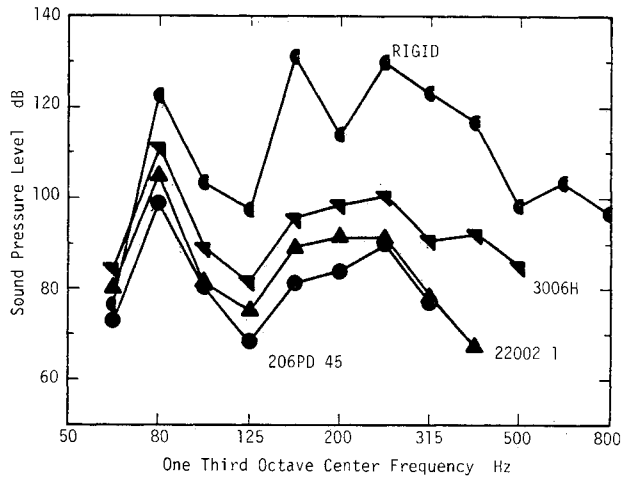

Fig 9 Comparison of SPL spectra for various isolators, 2640 rpm

The experimental force excitation levels could not be ad justed to the high levels used in the design model To correct this difference in sources, input force to interior sound pressure level response transfer functions were computed from the time correlated records of the drive and response signals Since the spectra were primarily discrete tones the transfer functions were computed only at the tones which were precisely identified in the drive signal spectrum Sample averaging was used via power and cross spectra calculations to enhance the data It was found that the peak transfer functions in the spectrum were well represented using only one sample average while the lower transfer function values were well represented within three sample averages

To determine if a facility noise floor was reached during the isolator evaluation a special airborne configuration run was made The dummy engine was connected to the shaker and supported by a "sky hook " an overhead crane while the tire pressure in the aircraft was reduced to lower the aircraft to its engine installed attitude In effect the structure borne noise path was cut and the airborne noise path reconstructed as in the isolator installed configurations The only difference in the configurations would be the engine static loading effects on the fuselage airframe response Transfer function data were obtained at each of the five engine speed settings and interior noise spectra computed based on the force excitation levels used in the design model evaluations The airborne component levels were considered sufficiently high to warrant removal of this component from the isolator data This was accomplished by comparing at each tone in the spectrum the measured airborne and isolator data components at each microphone location If the isolator data were 6 dB greater than the airborne component, the two levels were subtracted to obtain the structure borne component The spectrum frequency at which the isolator data were less than 6 dB above the airborne component was considered to be the useful frequency range of measured data and all data above that frequency were no longer considered in the OASPL com putations

Analysis and Results

Typical comparison of one third octave maximum sound pressure level spectra is given in Fig 9 In general decreasing the isolator stiffness decreases structure borne noise trans mission throughout the spectrum; however not necessarily uniformly As expected the largest decrease in noise trans mission occurred when going from the rigid isolator con figuration to the original equipment 3006H isolator con figuration; however the exceptionally large difference ob tained at the simulated engine speed of 2740 rpm was quite surprising For the nonrigid isolator configurations the unweighted spectra are dominated by the response in the 80 Hz one third octave band The 80 Hz band spans the frequency range from 70 8 to 89 1 and thus contains the fourth engine harmonic (72 88 Hz) which has the highest drive level of any tone in the input drive spectrum

Unweighted and A weighted maximum overall sound pressure level data are listed in Table 3 for all isolator con figurations at each of the five simulated engine speeds The one third octave band beyond which the measured data were no longer 6 dB above the airborne noise levels f_{BAND} is also given in the table to indicate the useful range of measurement for the given isolator configuration As can be seen by the data listed in Table 3 the airborne noise transmission did not greatly influence the unweighted OASPL data; however it had a noticeable influence on the A weighted levels par ticularly for the softer isolator configurations which exhibited overall lower transmission levels

Table 3 Comparison of measured peak overall sound pressure levels

Isolator	rpm	OASPL, dB	OASPL, dB(A)	f_{BAND}, Hz
3006H	2160	111 2	94 7	500
	2280	116 7	96 4	630
	2400	112 6	93 3	250
	2520	111 6	95 3	250
	2640	111 9	96 8	500
Rigid	2160	129 7	114 5	800
	2280	129 5	108 8	800
	2400	123 9	109 2	800
	2520	121 7	106 4	800
	2640	134 5	124 9	800
22002 1	2160	103 7	89 1	500
	2280	113 0	91 1	315
	2400	107 9	87 6	200
	2520	105 4	87 5	200
	2640	105 6	88 3	400
WRB 030M	2160	106 5	91 1	315
	2280	114 1	92 4	200
	2400	110 3	89 8	200
	2520	109 3	94 7	250
	2640	104 0	90 2	250
22002 11M	2160	107 9	89 3	315
	2280	110 7	90 2	250
	2400	109 4	93 6	250
	2520	108 3	92 2	250
	2640	107 9	95 8	250
206PD 45	2160	96 7	81 2	200
	2280	106 3	85 1	250
	2400	104 3	83 3	200
	2520	101 8	84 2	200
	2640	99 7	84 3	315

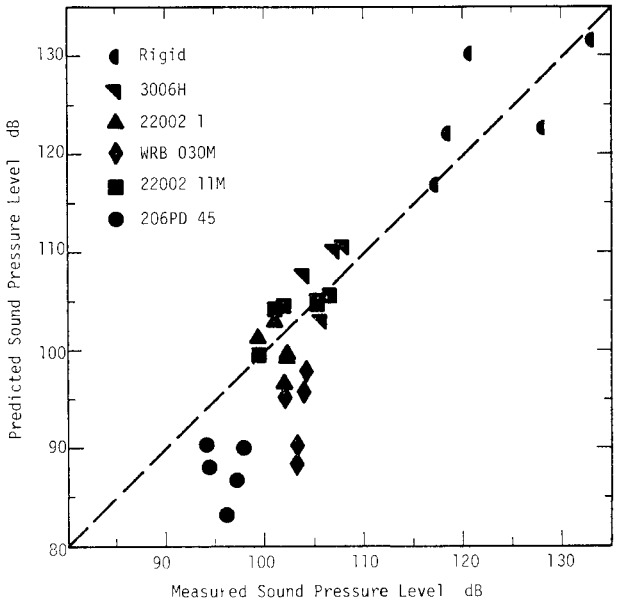

Fig 10 Correlation of design model predictions to measured un weighted OASPL

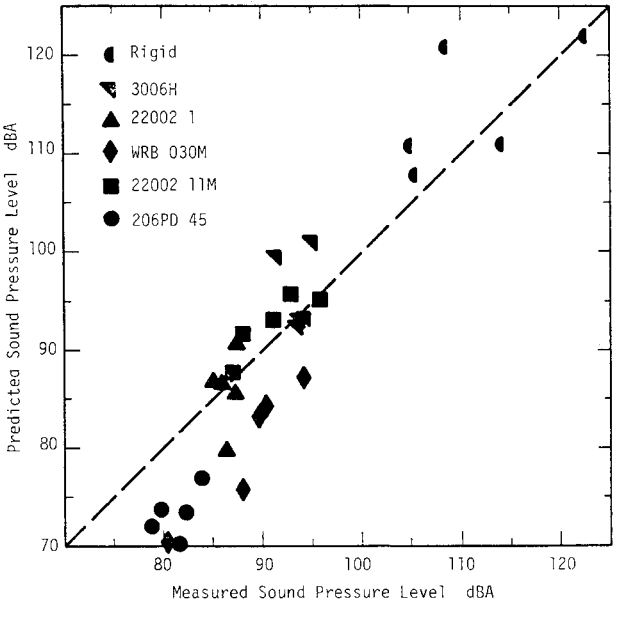

Fig 11 Correlation of design model predictions to measured A weighted OASPL.

By comparing the maximum unweighted OASPL level of 116 7 dB for the original 3006H equipment isolators to the maximum level of 106 3 dB for the 206PD 45 isolator con figuration it can be seen that 10 4 dB noise level reduction was accomplished during the investigation Likewise an A weighted noise level reduction of 11 7 dB(A) was realized

Comparison of Test Results with Design

The overall structure borne noise level reductions fell somewhat short of the 15 dB design goal originally chosen for the program, which warranted a more detailed analysis of the test data and design model procedures Detailed analysis of the test data revealed that the aft cabin microphone (P3) was not repositioned correctly during the noise transmission tests which lead to measurably higher SPL responses Un fortunately P3 also controlled the maximum cabin levels This discovery prompted the removal of P3 from the test data and reanalysis of the isolators using the design model with P3 removed from the maximum predicted cabin response

The measured isolator properties in the form of the design model parameters ($\bar{K}_A$ β L_R and η as taken from Table 2) were used in the design model to generate predictions for direct comparison to the measured OASPL data The measured and predicted unweighted and A weighted OASPL values for each of the isolator configurations at each of the five engine speeds are presented in the form of correlation plots as given in Figs 10 and 11 respectively As can be seen the correlation of predicted to measured values shows a conservative trend in the predicted levels The WRB 030M and 206PD 45 isolator configurations were somewhat un conservatively predicted; however they became much im proved when compared to the predictions using all three microphones [7] The A weighted spectrum levels show im proved correlation over those of the unweighted levels

It is of interest to note that the WRB 030M and 206PD 45 isolators were configured from much smaller volumes of elastomeric material than the other soft isolators (22002 1 and 22002 11M) and thus the level of dynamic strain per unit volume of elastomer would naturally be much higher The potential for these isolators to operate in a region of nonlinear elastic response due to excessive strain is much increased over that of the larger isolators Also it must be recalled that the effects of bidirectional static loading on the dynamic properties of the isolators were not determined and therefore may have been the reason for poor correlation of the WRB 030M and 206PD 45 isolators

Conclusions

An engine induced structure borne interior noise trans mission model for a single general aviation aircraft was used to develop a set of retrofit vibration isolator design curves for reduced interior noise transmission Several candidate isolator configurations were developed with the design objective of a 15 dB decrease in overall structure borne interior noise transmission over that of the aircraft's original equipment isolators Results from laboratory test evaluation of the candidate isolator configurations using simulated pure tone engine excitation support the following conclusions: 1) overall maximum interior noise level reductions on the order of 10 dB were realized from the candidate isolators when considering both forward and aft cabin noise levels and 2) the structure borne noise transmission model used in the isolator design specification was adequate for assessing the trends in improved structure borne noise isolation for a given change in isolator dynamic properties

Acknowledgments

This investigation was supported by NASA Langley Research Center under Contract NAS1 14861 Assistance by Dennis C Scheidt during laboratory data acquisition is gratefully acknowledged

References

[1]Unruh J F and Scheidt D C Engine Induced Structural Borne Noise in a General Aviation Aircraft ' *SAE Transactions* Vol 88 1980 pp 2171 2184

[2]Unruh, J F Scheidt D C and Pomerening D J Engine Induced Structural Borne Noise in a General Aviation Aircraft NASA CR 159099 Aug 1979

[3]Unruh J F Finite Element Subvolume Technique for Struc ture Borne Interior Noise Prediction *Journal of Aircraft* Vol 17 June 1980 pp 434 441

[4]Unruh J F Structure Borne Noise Prediction for a Single Engine General Aviation Aircraft *Journal of Aircraft* Vol 18 Aug 1981 pp 687 694

[5]Unruh J F and Scheidt D C Engine Isolation for Structure Borne Interior Noise Reduction in a General Aviation Aircraft NASA CR 3427 May 1981

[6]Unruh J F Procedure for Evaluation of Engine Isolators for Reduced Structure Borne Interior Noise Transmissions AIAA Paper 81 1970 Palo Alto Calif Oct 1981

[7]Unruh J F and Scheidt D C , Design and Test of Aircraft Engine Isolators for Reduced Interior Noise NASA CR 166021 Dec 1982

[8] Cessna 1963 Model 172D Skyhawk and Powermatic Series Owner s Manual Cessna Aircraft Co Wichita Kansas Aug 1975

[9]Snowdon J C Handbook of Vibration and Noise Control Applied Research Laboratory The Pennsylvania State University University Park Pa Rept AD/A 071 485 April 1979